21st Australasian Fluid Mechanics Conference
Adelaide, Australia
10-13 December 2018

Application of High-order Lattice Boltzmann for Binary Diffusive Mixing in Microfluidics: Comparison against Fluorescent Microscopy

C. S. From[1], E. Sauret[1], S. A. Galindo-Torres[2], M. Hejazian[3,4], Z. R. Li[5], N.-T. Nguyen[3] and Y.T. Gu[1]

[1]School of Chemistry, Physics, and Mechanical Engineering, Science and Engineering Faculty, Queensland University of Technology, QLD 4001, Australia

[2]Department of Civil Engineering and Industrial Design, University of Liverpool, Liverpool L69 3BX, UK

[3]Queensland Micro- and Nanotechnology Center, Griffith University, QLD 4111, Australia

[4]ARC Centre of Excellence for Advanced Molecular Imaging, Department of Chemistry and Physics, La Trobe Institute for Molecular Sciences, La Trobe University, VIC 3086, Australia

[5]College of Mechanical and Electrical Engineering, Wenzhou University, Wenzhou 325035, China

Abstract

Diffusive mixing between miscible fluids is an important process in many microfluidic applications, especially for biological studies. In microfluidic experiments it is common to observe microscopic fluid dynamics through fluorescence microscopy. Applying this technique to a hydrodynamic focusing device with a core-flow containing ferrofluid and fluorescence, an unexpected physical phenomenon referred to as the 'saddle-like' distribution was observed. Lattice Boltzmann (LB) methods have recently gained tremendous popularity as a numerical approach to model microfluidic dynamics. Despite the recent advancements in LB, reports on the application of high-order LB methods to single-phase miscible mixtures in microfluidics have been limited. The work presented here focuses on the application of high-order LB models to the simulation of single-phase binary miscible mixtures in microfluidic systems. We demonstrate the ability of our numerical simulation to capture the characteristics of the 'saddle-like' phenomenon and highlight the difficulties and limitations faced when comparing numerical results against experimental fluorescence microscopy with ferrofluids. This work sets the preliminary steps towards a LB model for simulating fluid mixtures in micro- and nanofluidics and allows for future advancements through higher order expansions.

Introduction

Over the past decade, micro- and nanofluidics have shown potential as fully functional miniaturized devices. The potential applications of such devices have resulted in a substantial gain in interest by a variety of research fields including the medical and resource industries. Fluid mixtures are present in many microfluidic applications, e.g., biological samples can contain multiple fluid species. Mixtures present physical complexity given that constituent species all have different transport properties and thereby impose different fluid flow characteristics [9, 8]. In microfluidic experiments it is common and convenient to observe microscopic fluid dynamics through fluorescence microscopy, which typically use sodium fluorescein salt molecules. In micromixers where fluid mixtures are homogeneous, constituent species concentrations are identified by the various light intensities emitted by the sodium fluorescein salt molecules, which have their own individual transport properties. Such complexity is illustrated in the pressure-driven technique named hydrodynamic focusing that is commonly used to achieve high-throughput micromixers. To incorporate hydrodynamic focusing, microfluidic channels are configured with T or Y-junctions, or both [15], where the streaming fluids from these junctions impose a pressure and mix fluids. From the literature, it is known that, in hydrodynamic focusing for flow containing multiple species, the faster diffusing fluid will diffuse across the interface of the slower diffusing fluid, resulting in an inter-diffusion region that consist of a mix between the two fluid streams [9]. For fluids with different weights, the lighter fluid diffuses into the heavier fluid [8]. The heavier fluid will not deviate far from its original stream since pressure-driven diffusion has a dominating effect over the molecular diffusion [8, 7]. In recent work by [6] the concept of hydrodynamic focusing was applied for magnetofluidic micromixer to achieve high mass-flow rates at high mixing efficiency. In their work, the focused core-flow contained both ferrofluid and fluorescence. Using fluorescence microscopy, it was observed that light-intensity peaked at the outer edges of the illuminated focused core-flow, forming a saddle-like distribution, shown in figure 1, rather than the standard error-function distribution of diffusive mixing. This behaviour was unexpected and is currently a new and unexplored phenomenon in hydrodynamic focusing. There is currently no numerical model so far that is capable of reproducing this complex flow phenomenon experimentally observed by [6]. Previous work by [7] investigated a similar phenomenon using confocal imaging, however, in their study the phenomenon was due to fluids diffusing in the transverse direction as a result of the channel thickness. In [6] the thickness (short-transverse) of the channel is one tenth of the width (long-transverse) and therefore we suspect that the short-transverse diffusion has minimal effect.

Understanding the physical phenomenon in these fluidic devices is a necessity for optimizations, and therefore, is an essential aspect to future advancements in microfluidics [2]. Hydrodynamic numerical simulations have the ability to describe such phenomenon and provide detailed description of transport properties that are not observable and quantifiable through experimentation [1]. Recently, the Lattice Boltzmann (LB) method has gained tremendous popularity, due to its accuracy, adaptability and scalable parallel computations [1]. LB is also an attractive alternative to Navier-Stokes (NS) based numerical methods for simulating microfluidic applications [1]. It is known that Higher-order LB models have the ability to describe hydrodynamics that is beyond NS capabilities [14]. Therefore, LB methods have the potential to be used as an alternative to computationally expensive atomistic methods such as Direct Simulation Monte Carlo [10]. The development of multi-component models have extended the capabilities of LB methods to solve complex fluid systems that involve multiple fluids. In the context of this work we are interested in pseudo-potential method, generally referred to as the Shan-Chen (SC) model, which have consistently been shown to accurately reproduce complex multi-component systems [3, 4].

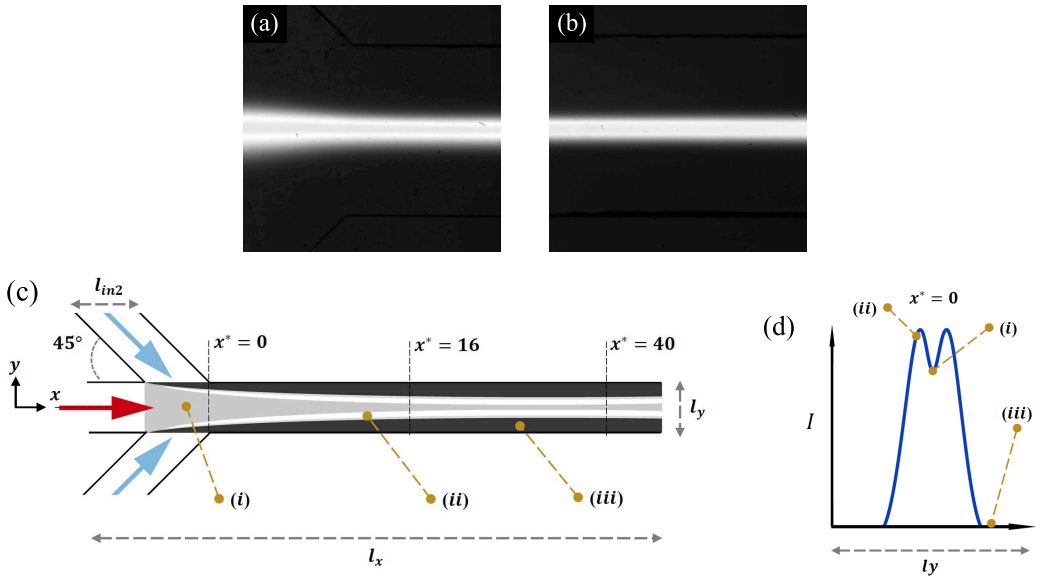

Figure 1: Experimental fluorescence microscopy image (based on work from [6]) at approximate cross-sections ($x^* = 2x/l_y$): (a) entry $x^* = 0$ and (b) $x^* = 16$ middle of the channel. (c) Micro-channel 2D schematic and illustration of the hydrodynamic focused flow where Arrows define: $\rightarrow$ sheath-flow and $\rightarrow$ core-flow. (d) is a graphic representation of the saddle-like distribution of intensity (I) concentration. Marked regions define: (***i***) FF+F_{dye}+ DI-water, (***ii***) F_{dye}+DI-water and (***iii***) DI-water. (NOTE: images are not scaled relatively and experimental images (a) and (b) have been brightened for improved illustration purposes.)

Experimental Hydrodynamic focusing in microfluidic device

In Hejazian *et al,* [6] hydrodynamic focusing was achieved in a magnetofluidic micromixer with a Y-junction configuration presented in figure 1. The phenomenon of interest is the saddle-like shape seen in the hydrodynamic focused core-flow in figure 1. Refer to [6] for the physical parameters used in this work. In their work, the core-flow mixture, indicated as (***i***) in figure 1 (c) consists of DI-water with two primary components. The first is a commercial sodium fluorescein, SIGMA-ALDRICH F6377 ($C_{20}H_{10}Na_2O_5$). The second component consists of ferrofluid (FF), a commercial product (Ferrotec EMG707) that contains 10 nm Magnetite (Fe_3O_4) nanoparticles diluted in DI-water at concentration of 2% volume and is completely solute (opaque liquid colour). The core-flow mixture contains 0.05 g of sodium fluorescein which is mixed in 20 mL of deionized water (DI-water). The FF is diluted with the mixture to 20% volume concentration. Molecular mass of these two components are $m_{C_{20}H_{10}Na_2O_5} = 376.27$ g mol^{-1} and $m_{Fe_3O_4} = 231.53$ g mol^{-1}, and DI-water (H_2O) takes the general value of $m_{H_2O} = 18.015$ g mol^{-1}. We will refer to parts of the core-flow mixture as two individual components, the first DI-water+ 0.05 g of sodium fluorescein as F_{dye} and the diluted ferrofluid at 20% volume as FF. The saddle-like distribution posses a number of properties which we will briefly introduce here: The molecular mass of FF and F_{dye} are more than a magnitude heavier than the carrier medium (DI-water), which impose a pressure from the sheath flows on the core-flow and thereby results in the thin focused stream [8]. However, the saddle-like distribution peaks correspond to I= 1 (region (***ii***) in figure 1), which based on the calibration by [6] indicate that at these locations there is a near complete absence of FF. This means that despite prior mixing of the FF and F_{dye}, they separate as an effect of their individual transport properties and the sheath flow.

LB model for miscible mixtures in microfluidic flows

In the lattice Boltzmann method, mesoscopic representation of fluid flow is described by the distribution function, f. In this work an athermal third-order equilibrium distribution function (third-order Hermite polynomial expansion) is developed following the seminal work by [14], to comply with NS level of description of hydrodynamics, more specifically, the momentum dynamics and pressure tensor. A general rule for matching the order of equilibrium distribution (M) to the algebraic degree of precision of the velocity-set (N) is $N > 2M$ [14], hence to retain the third-order level of detail of the equilibrium function an algebraic degree of precision of N=7 is required. For this reason we use the two-dimensional 17-velocity lattice structure (D2Q17), which is, to the authors' knowledge, the shortest lattice velocity set to satisfy this requirement [14, 12]. The lattice distribution f in space x, in each discrete velocity ξ_α of all 17 directions α, at time t for one fluid (σ) has the following evolution,

$$f_\alpha^\sigma(x+\xi_\alpha, t+\Delta t) = f_\alpha^\sigma(x,t) - \Omega_\sigma + \Delta t \mathrm{f}_\alpha^{F,\sigma}(x,t). \tag{1}$$

The first term in the above equation (1), $f_\alpha^\sigma(x+\xi,\, t+\Delta t)$, is the constant propagation of particles in space x at each time interval Δt. This is the streaming step. The far-right hand term in equation (1) is the forcing term which is added to include intermolecular interaction forces to the collision process. This is coupled explicitly to the distribution function to conserve the explicit nature of LBM by [5],

$$\mathrm{f}_\alpha^{F,\sigma} = \frac{F^\sigma(\xi_\alpha - u')}{m_\sigma n_\sigma c_s^2} f_\alpha^{eq(\sigma)}, \tag{2}$$

where the explicit form of the distribution requires the transformation $\tilde{f}_\alpha^\sigma(x,t) = f_\alpha^\sigma(x,t) - \frac{\Delta t}{2}\mathrm{f}_\alpha^{F,\sigma}(x,t)$. We will omit $\tilde{f}$ and simply refer to the distribution by f. The collision term Ω_σ in equation (1) traditionally reads in the form of single-relaxation model,

$$\Omega_\alpha^\sigma = \left[\frac{1}{\tau_\sigma}\left(f_\alpha^\sigma(x,t) - \frac{\Delta t}{2}\mathrm{f}_\alpha^{F,\sigma}(x,t) - f_\alpha^{eq(\sigma)}(x,t)\right)\right], \tag{3}$$

which relaxes the distribution using the relaxation parameter τ based on the kinematic viscosity ν of the fluid, i.e. $\nu_\sigma = c_s^2 \cdot (\tau_\sigma - 1/2)\frac{\Delta x^2}{\Delta t}$, where on a discrete lattice $\Delta x = \Delta t = 1$. The sound

speed is based on the lattice, for D2Q17 $c_s = \frac{1}{\sqrt{(125+5\sqrt{193})/72}}$.
Following [14] the systematic procedure to derive higher order LB models by expansion of Hermite polynomials, the third-order expansion yields:

$$f_\alpha^{eq(\sigma)} = w_\alpha n_\sigma \left\{ 1 + \underbrace{\frac{\xi_\alpha \cdot u_\sigma}{c_s^2}}_{1^{st}\text{ Order}} + \underbrace{\frac{1}{2}\left[\left(\frac{\xi_\alpha \cdot u_\sigma}{c_s^2}\right)^2 - \frac{u_\sigma^2}{c_s^2}\right]}_{2^{nd}\text{ Order}} + \underbrace{\frac{\xi_\alpha \cdot u_\sigma}{6\cdot c_s^2}\left[\left(\frac{\xi_\alpha \cdot u_\sigma}{c_s^2}\right)^2 - 3\frac{u_\sigma^2}{c_s^2}\right]}_{3^{rd}\text{ Order}} \right\}. \tag{4}$$

We point out that from equations (2), (3) and (4) we retain accuracy of the third-order equilibrium in the forcing term during the collision. The number density n_σ at each lattice site in space x is defined by summation of distribution f_α^σ in all directions α. Momentum is then computed by the sum of $f_\alpha^\sigma \cdot \xi_\alpha$ and the additional force contribution,

$$n_\sigma = \sum_\alpha^Q f_\alpha^\sigma \xi_\alpha, \quad \rho_\sigma u_\sigma = m^\sigma \sum_\alpha^Q f_\alpha^\sigma \xi_\alpha + \frac{\Delta t}{2} F_\sigma. \tag{5}$$

Mass density can be defined by the conventional description $\rho = n \cdot m$. The mass of each component and total momentum for a system of S number components is conserved respectively by satisfying the following,

$$\sum_\alpha^Q \Omega_\alpha^i = 0,\ i = \sigma, ..., S, \tag{6a}$$

$$\sum_i^S m_i \sum_\alpha^Q \Omega_\alpha^i \xi_\alpha = 0. \tag{6b}$$

where, the collide stream process, equations (1), (3) and (5), will ensure mass (6a) is conserved. However, to satisfy total momentum conversation (6b), u in equation (4) needs to be replaced with the *common* mixture velocity [13]

$$u' = \frac{\sum_i^S (m_i n_i \cdot u_i)(\tau_v^i)^{-1}}{\sum_i^S m_i n_i (\tau_v^i)^{-1}}. \tag{7}$$

Furthermore, the total velocity of the fluid mixture (barycentric velocity) is defined by $u_T = \frac{\sum_i^S (m_i n_i \cdot u_i)}{\sum_i^S m_i n_i}$.
The force tensor in the SC multi-component model due to inter-particle interactions is defined by [13]

$$F_\sigma = -\psi_\sigma(x) c_s^2 \sum_i^S G_{\sigma i} \sum_\alpha^Q w_\alpha^f(|e_\alpha|^2) \psi_i(x + e_\alpha) e_\alpha, \tag{8}$$

where $w_\alpha^f(|e_\alpha|^2)$ represents weights for the forcing term and G is the interaction strength between components, which can essentially be used as a control variable. In this work we set G below the immiscible limit for binary single-phase miscible mixtures. To avoid spurious currents due to insufficient isotropy gradient equation (8) [see [11]], we use an eight-order isotropy model.

Numerical Results and Discussion

We compare our results against the light intensity (I^*) measurements [6]. A numerical equivalent of I^*, which we call *pseudo*-light intensity, is obtained by considering the saddle-like distribution to be the superposition of two Gaussian curves; a positive intensity by F_{dye} and an adverse intensity due to the opaque FF. All numerical simulations are carried out on a converged symmetric grid ($N_y = 150$ and $N_x = 1200$). Physical quantities have been converted to dimensionless lattice units based on this grid size and the D2Q17 lattice sound speed. Refer to [6] for physical quantities. We have used half-way bounce-back boundary conditions on the walls to ensure *no-slip* condition. Velocity bounce-back is applied at inlet to conserve mass and momentum and a zero gradient convective boundary condition at outlet.
The developed LB model is in excellent agreement with experimental data, as seen in figure 2, accurately predicting the concentration profile of the squeezed core-flow. The width of the thin concentration profile is accurately defined along y^*. Peak intensities are accurately reproduced by the model, measuring 4.3624×10^{-5} m at both $x^* = 0$ and $x^* = 16$ compared with experimental 4.28×10^{-5} m. This an error of $\pm 1.9252\%$, which likely due to spatial resolution. The model is capable of reproducing convective diffusion which dominates the fluid motion of both core-flow components F_{dye} and FF in the longitudinal direction since the core-stream maintained with a dissipating saddle-distribution, as seen in figure 2. We can see that the saddle-like distribution has a strong adverse-intensity at cross-sections $x^* = 0$ that is much more pronounced than experimentally observed. However, notice that the adverse-intensity then slowly decays further down the channel at $x^* = 16$, which coincide with experimental profiles. Over a longer distance, $x^* = 0 \rightarrow 16$, the diffusion of F_{dye} and FF will cause a more pronounced inter-diffusion for which these two fluids mix broadening the width of the profile and thereby decrease the saddle depth. To demonstrate numerical and experimental agreement we measure the expansion ratio in profile width between $x^* = 0$ and $x^* = 16$ at the lower end $I^* = 0.03$ in figure 2. Our model numerically predict the width to expand at a ratio $= 1.4829$ in close agreement with experimental measure ≈ 1.456. This confirms that the concentration of all three fluids in the short-transverse diffusion (along the channel depth) are uniform and do not contribute to the saddle phenomenon observed, at least not to any significant degree. We defer more in depth investigations to future work.

Discrepancy between Experimental and Numerical Results

There are, admittedly, some differences present between the model and experiments, as highlighted by close up views in figure 2. In particular, the depth of saddle-like distribution profiles at both $x^* = 0$ and $x^* = 16$, as seen in figure 2, is significantly more pronounced in numerical results than experimentally observed. These discrepancies are due to the combination of numerical and experimental uncertainties, which are to be expected but are more susceptible due to the small physical size of micro-device and the fact that the application is dynamic, rather than static. The numerical uncertainties surround the pseudo-light intensity I^* where our current approach assume the normalized adverse-intensity to be linearly proportional to the ferrofluid mixture concentration. However, this is not with exact certainty since in the experimental data there is uncertainty associated with potential luminescence quenching of magnetite and fluorescence. We stress that correlating numerical simulations with experimental results in the form of light intensity is not easily achieved due to the opaqueness of the ferrofluid and the fact that the light emitted (photons) are not simulated directly. In addition, transport properties of ferrofluid may differ from specified values in Material Data Sheet. Considering all these factors, we emphasise that the numerical results are in qualitative agreement to an acceptable level of deviation with experimental data and most importantly that the underlying characteristics of the phenomenon is reproduced numerically.

Conclusions

In this work we numerically simulated the physical phenomenon

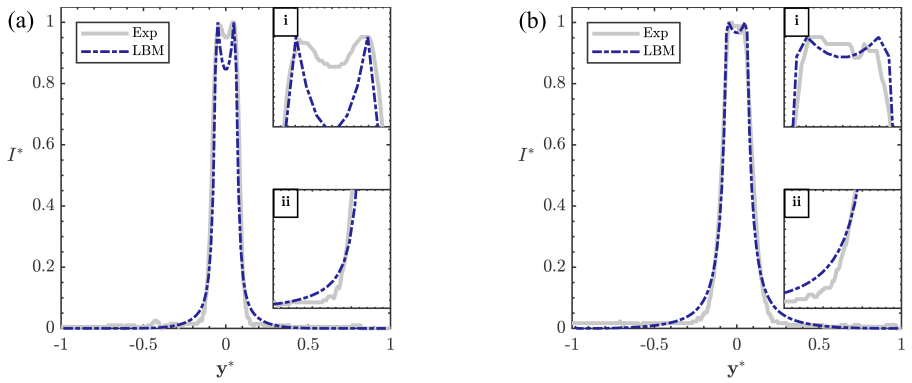

Figure 2: Normalized experimental light intensity profiles [6] compared against numerical *pseudo*-light intensity I^* at (a) $x^* = 0$ and (b) $x^* = 16$. Close-up views (i) the saddle shape [y^*(-0.08;0.08), I^*(0.8;1.05)] and (ii) the profile width [y^*(-0.3;0.0), I^*(0.0;0.25)].

'saddle-like distribution' observed experimentally in [6] magnetofluidic micromixer, in which diffusive mixing is achieved through hydrodynamic focusing. We presented methods and strategies involved in applying and developing a high-order LB model to simulate miscible binary single-phase mixtures in microfluidic. Specifically, an equilibrium distribution function expanded to third-order was used in conjunction with the high-order lattice structure D2Q17 to completely resolve NS level of detail for hydrodynamics (athermal). We demonstrated that the model is capable of reproducing the underlying characteristics of the saddle-like distribution phenomenon. Both numerical and experimental uncertainties were highlighted and discussed to provide insight into the challenges faced in modelling the diffusive mixing of binary mixtures. A more in depth investigation is required to address these uncertainties. In particular, additional fluorescence microscopy experiments are required to confirm if the adverse intensity due to opaque ferrofluid is linearly proportional to its concentration. If not, then it is possible that quenching process occurs. Nonetheless, the work here constructs the basis of a preliminary high-order lattice model that is capable of modelling single-phase binary miscible mixtures.

Acknowledgements

The authors acknowledge the High Performance Computing facilities at QUT and thank the QUT-HPC team for their support. Y-T. Gu and E. Sauret thank the Australian Research Council for its financial support under ARC Linkage LP150100737. Z.R. Li is supported by the National Natural Science Foundation of China (Grant Nos. 11372229, 21576130, 21490584). N.-T. Nguyen acknowledges funding support from Australian Research Council through the ARC linkage (LP150100153).

References

[1] Aidun, C. and Clausen, J., Lattice-boltzmann method for complex flows, *Annual Review of Fluid Mechanics*, **42**, 2010, 439–472.

[2] Bocquet, L. and Tabeling, P., Physics and technological aspects of nanofluidics, *Lab Chip*, **14**, 2014, 3143–3158.

[3] Chen, L., Kang, Q., Mu, Y., He, Y.-L. and Tao, W.-Q., A critical review of the pseudopotential multiphase lattice boltzmann model: Methods and applications, *International Journal of Heat and Mass Transfer*, **76**, 2014, 210 – 236.

[4] Galindo-Torres, S., Scheuermann, A., Li, L., Pedroso, D. and Williams, D., A lattice boltzmann model for studying transient effects during imbibition–drainage cycles in unsaturated soils, *Computer Physics Communications*, **184**, 2013, 1086 – 1093.

[5] He, X., Shan, X. and Doolen, G. D., Discrete boltzmann equation model for nonideal gases, *Phys. Rev. E*, **57**, 1998, R13–R16.

[6] Hejazian, M., Phan, D.-T. and Nguyen, N.-T., Mass transport improvement in microscale using diluted ferrofluid and a non-uniform magnetic field, *RSC Adv.*, **6**, 2016, 62439–62444.

[7] Ismagilov, R. F., Stroock, A. D., Kenis, P. J. A., Whitesides, G. and Stone, H. A., Experimental and theoretical scaling laws for transverse diffusive broadening in two-phase laminar flows in microchannels, *Applied Physics Letters*, **76**, 2000, 2376–2378.

[8] Kamholz, A. E., Weigl, B. H., Finlayson, B. A. and Yager, P., Quantitative analysis of molecular interaction in a microfluidic channel: the t-sensor, *Analytical Chemistry*, **71**, 1999, 5340–5347.

[9] Knight, J. B., Vishwanath, A., Brody, J. P. and Austin, R. H., Hydrodynamic focusing on a silicon chip: Mixing nanoliters in microseconds, *Phys. Rev. Lett.*, **80**, 1998, 3863–3866.

[10] Meng, J. and Zhang, Y., Gauss-hermite quadratures and accuracy of lattice boltzmann models for nonequilibrium gas flows, *Phys. Rev. E*, **83**, 2011, 036704.

[11] Sbragaglia, M., Benzi, R., Biferale, L., Succi, S., Sugiyama, K. and Toschi, F., Generalized lattice boltzmann method with multirange pseudopotential, *Phys. Rev. E*, **75**, 2007, 026702.

[12] Shan, X., General solution of lattices for cartesian lattice bhatanagar-gross-krook models, *Phys. Rev. E*, **81**, 2010, 036702.

[13] Shan, X., Multicomponent lattice boltzmann model from continuum kinetic theory, *Phys. Rev. E*, **81**, 2010, 045701.

[14] Shan, X., Yuan, X.-F. b. and Chen, H., Kinetic theory representation of hydrodynamics: A way beyond the navier-stokes equation, *Journal of Fluid Mechanics*, **550**, 2006, 413–441.

[15] Suh, Y. K. and Kang, S., A review on mixing in microfluidics, *Micromachines*, **1**, 2010, 82–111.